Removal Of Ciprofloxacin From Waste Water By Photocatalytic Method With Waste Polystyrene And Tio_2 Composites

Hayrı-Senel T.[1*], Kahraman E.[1], Sezer S.[1], Erdol-Aydın N.[1], Nasun-Saygılı G.[1]

[1]Istanbul Technical University, Faculty of Chemical and Metallurgical Engineering, Department of Chemical Engineering

*corresponding author
e-mail: hayri16@itu.edu.tr

Abstract Ciprofloxacin (CIP) is one of the widely used antibiotics. Since ciprofloxacin in the aquatic ecosystem adversely affects human health as well as other organisms, it must be removed from wastewater.
The aim of this study was to develop polystyrene (PS) and TiO_2 composites that can be used as catalysts in CIP removal by photocatalytic process. Waste PS was used in these composites. This is important in terms of the use of one waste in the removal of another waste.
This process is optimized using Box-Behnken Design. Parameters such as the amount of polymer in the composite, pH and initial CIP concentration were studied and their effects on CIP removal were investigated.
The validity and adequacy of the selected model were evaluated according to the relevant statistical data. These are R^2= 0.9751, adjusted R^2=0.9565, the model's p-value <0.0001 and the lack of fit-value 0.246. In the process carried out under optimum conditions, the CIP removal was found to be 95.01% at the end of 180 minutes. This value was predicted as 94.37% in the model. According to these results, it was seen that the model represents the real process with high accuracy.
Keywords: Ciprofloxacin, waste polystyrene, TiO_2, photocatalyst

1. Introduction

Ciprofloxacin (CIP) is a fluoroquinolone antibiotic with a broad antimicrobial spectrum. It can be used for many diseases such as digestive and urinary tract infections, various skin and lung diseases [1,2]. Over the years, the concentration of antibiotics in water bodies has increased [1]. Considering the significant detection of ciprofloxacin in aquatic environments, the necessity of removing it from wastewater emerges. In the literature, there are studies on the removal of ciprofloxacin from wastewater [2–6]. One of the most common techniques used for this purpose is the photocatalytic degradation of ciprofloxacin [1,7].

Titanium dioxide, TiO_2, is an abundant, stable, economical, efficient photocatalyst that is widely used due to its high catalytic activity, high oxidizing power, and high photocorrosion resistance. TiO_2 can be used in wastewater studies in powder form, or it can be used in combination with suitable substrates. However, some problems arise when used in powder form. One of these problems is that recovery of the catalyst after application is difficult, time consuming and expensive. The most widely used way to overcome these disadvantages is the immobilization of TiO_2 with various substrates [3,5,8–10].

Polystyrene (PS) is a support material that can be preferred due to its inert structure, ease of production, low cost and ability to float in water. Plastic waste is a worldwide environmental problem. One of the commonly encountered plastic wastes is PS waste. It is very important to use these PS wastes for the removal of pollutants in different environments [9].

Various statistical and mathematical methods are used to analyze different chemical processes, to save time, to predict and simulate the conditions in this process. One of the most common methods used for this purpose is Response Surface Methodology (RSM), Box-Behnken Design [11].

In this study, first of all, PS-TiO_2 composites were synthesized and their removal performances were investigated by using them as a catalyst in the photocatalytic degradation of CIP from wastewater. The Box-Behnken Design was chosen to analyze the degradation process of CIP, and to optimize the effective parameters. MINITAB software version 21.0 was used for the experimental design.

2. Materials and Methods

2.1. Materials

Waste PS was collected from used waste spoons. TiO_2 (anatase,powder 99.8%), chloroform and ethanol were purchased from Merck.

2.2. Characterization

X-Ray Diffraction (XRD) analysis was performed using the PANalytical XPert Pro device for the structural evaluation of anatase TiO_2, waste PS and PS-TiO_2 (1.5406 Å for 2θ ranging from 10° to 90°). The surface morphology of waste PS and its composites were determined by Scanning Electron Microscope (SEM, QUANTA FEG250 Field Emission). Elemental analysis was performed using Energy dispersive analysis of X-ray (EDAX). Waste PS, TiO_2 and PS-TiO_2 composite were analyzed by FT-IR spectrophotometer (Bruker) in the range of 650 cm^{-1} to 4000 cm^{-1}.

2.3. PS-TiO_2 composite preparation

To form the PS-TiO_2 composite, a known amount of the polymer particles obtained from waste spoon and TiO_2 were placed in a beaker containing 1:8 ethanol and chloroform. This mixture was homogenized in a sonication water bath for 1 hour. It was then stirred at 120°C for 2 hours. The resulting solution was poured into a glass petri dish and kept in a fume hood for 24 hours for solvent evaporation. The resulting product was washed several times with distilled water in order to remove any impurities that may be on the product, and it was dried in an oven at 50°C for 24 hours[12]. This procedure was applied for all PS-TiO_2 products (Cx) containing different ratios of PS. Thus, C20, C50 and C80 composites were produced. The numbers in the names refer to the percent by weight PS in the composite.

2.4. Evaluation of photocatalytic efficiencies

The efficiency of the PS-TiO_2 photocatalysts was measured by the photocatalytic degradation of an aqueous ciprofloxacin solutions. Photodegradation studies were carried out under magnetic stirring at room temperature. In these studies, two LED daylight lamps were used as the light source. Ciprofloxacin solutions were prepared at different initial concentrations (C_0) (5, 10 and 15 mg/L). In a typical study, 20 mg of catalyst was added to 50 ml of ciprofloxacin aqueous solution. The mixture was then stirred in the dark for 30 minutes. Thus, the adsorption and desorption equilibrium of the mixture was achieved. While the mixing was continuing, the LED lamps were turned on and the concentrations of the samples taken from the medium were measured at certain time intervals. The samples were first filtered through a 0.20 mm PTFE membrane syringe filter and the absorbance values of the filtered solutions were determined at 277 nm with a UV-Vis spectrophotometer (Hach DR6000). Using these values, the percent degradation of ciprofloxacin was calculated according to Eq. (1). Here, C_0 and C_t represent the CIP concentration value at the start time (t_0) and the concentration values at any time (t), respectively.

$$CIP\ removal\ (\%) = ((C_0 - C_t)/C_0) * 100 \quad (1)$$

2.5. Experimental Design

3-factor and 3-level Box-Behnken design was used to optimize ciprofloxacin removal conditions. Analysis of the results was performed with Minitab software (Minitab 21.0). The effect of three factors (independent variables) on ciprofloxacin removal was examined at three different levels, including the amount of polymer in the composite (wt%) (A), ambient pH (B), and ciprofloxacin concentration in the initial solution (C) (Table1). The percent ciprofloxacin removal (dependent variable, Y) was determined as the response of the designed experiments. In this design used, 15 experimental studies were planned, including 3 center points. The significance of the variables was evaluated by analysis of variance (ANOVA, p-value<0.05), while the fit of the model was evaluated using R^2 and adjusted R^2 values. Data were fitted to obtain a quadratic polynomial. The conditions that achieved the highest CIP removal were considered as optimized conditions for this system.

Table 1: Factors and levels used in Box-Behnken design.

Factors	Symbols	Levels		
		Low -1	Medium 0	High 1
Amount of polymer (in composite, % by weight)	A	20	50	80
pH	B	3	7	11
Ciprofloxacin initial concentration (mg/L)	C	5	10	15

3. Results and Discussions

3.1. XRD analysis

Figure 1a shows the XRD pattern of anatase TiO_2. The sharp Bragg peaks indicate the highly crystalline nature of TiO_2. All characteristic peaks (2θ=25.53°, 38.1°, 48.35° and 54.18°) originating from the TiO_2 anatase phase are observed [13,14]. Looking at the XRD pattern for waste PS in Figure 1b, an amorphous polymeric structure is seen. The XRD pattern of the C50 composite is also shown in Figure 1c. This model confirms that amorphous phase is present in the compound due to PS. In addition, the broad peak at 2θ=20° corresponds to amorphous polystyrene. The characteristic peaks in Figure 1a are also seen here, confirming the presence of crystalline TiO_2 in C50[12].

3.2. SEM and EDAX analysis

The morphologies of waste PS, C20, C50 and C80 composites were observed by SEM. SEM images are given in Figure 2. Looking at the waste PS images in Figure 2a and b, it is seen that it exhibits a smooth and homogeneous structure. Again, the white dots appearing in the same SEM images can be interpreted as the residual solvent (chloroform) thought to be trapped in the polymeric materials [15]. SEM images of C80, C50 and C20 show that TiO_2 is evenly distributed in the polymeric matrix [12].

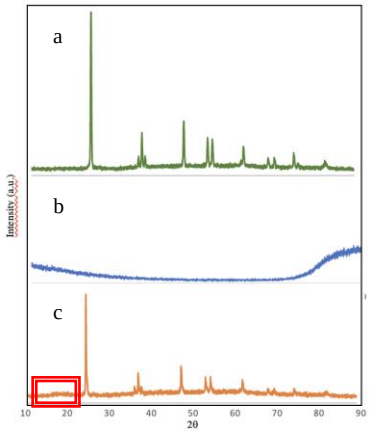

Figure 1. XRD patterns of a) anatase TiO_2, b) waste polystyrene, c) C50.

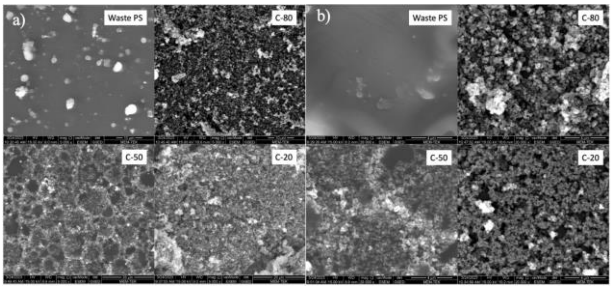

Figure 2. SEM images of waste PS, C80, C50 and C20 a) all images for mag=5000x b) all images for mag=20000x

Figure 3 shows the elemental mapping results of waste PS and its composites with different TiO_2 content (C80, C50 and C20). In addition, graphs showing the elemental density of the samples are embedded in the elemental mapping results of that sample. EDAX measurements show the distribution of element C, element O and element Ti in the polymer matrix[16]. Elemental mapping results confirmed that the composite with the highest TiO_2 (C20) contained more Ti elements than the rest of the composites, as expected, depending on its content.

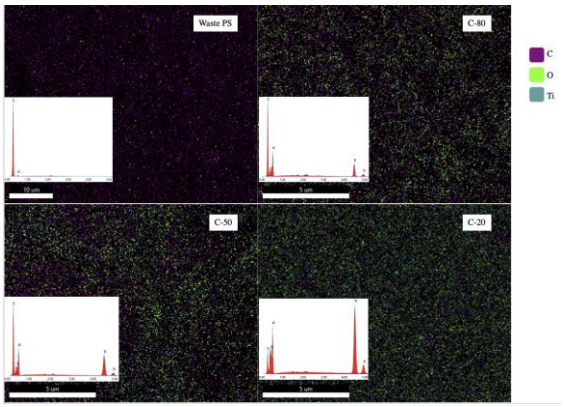

Figure 3. The elemental mapping results of waste PS and its composites.

3.3 FTIR Analysis

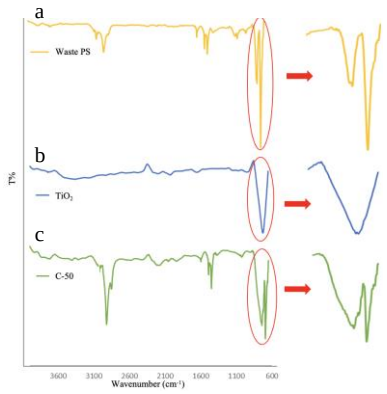

Figure 4. FTIR spectra of a) waste PS, b)TiO_2 and c)C50.

FTIR spectra of waste PS, TiO_2 and C50 are given in Figure 4. Looking at the IR spectra of waste PS, it is known that the peaks between 2800-3100 cm^{-1} originate from the C-H stretching vibration in the aromatic rings and the main chain. The peaks at 695, 748, 1027, 1451, 1492 and 1601 cm^{-1} belong to the C-H skeletal vibrations in PS. The peak seen in the TiO_2 spectra at 721 cm^{-1} is due to the O-Ti-O bonding in the form of anatase. In addition, the peaks appearing at 1660 cm^{-1} and 3375 cm^{-1} indicate surface adsorbed water and hydroxyl groups. The fact that all characteristic peaks appearing in both waste PS and TiO_2 are also visible in the spectra of C50 shows that TiO_2 can be successfully embedded into the PS polymer matrix[17].

3.4. Experimental design and optimization studies

The experimental design results according to Box Behnken were presented in Table 2 with the experimental measurement results and their predicted values. The minimum and maximum values of ciprofloxacin removal percentage were found to be 27 (R1) and 95 (R14), respectively. The results of the ANOVA test were shown in Table 3. After eliminating insignificant terms (p-value>0.05) from the model, the mathematical expression for the percent ciprofloxacin removal is as follows by Eq. (2).

$$Y = 58.29 - (10.5 * A) - (20.62 * B) - (8.37 * C) + (7.09 * B * B) - (5 * A * B) - (10 * A * C) \quad (2)$$

The R^2 value and the adjusted R^2 value were found to be 97.51% and 95.65%, respectively, ensuring the integrity of data. According to Table 3, the p value of the model is less than 0.05 and the p value calculated for the lack-of-fit is greater than 0.05 (F=3.38, p = 0.246) indicates that the significance level of the model is acceptable.

Table 2: Box-Behnken experimental design points and responses with their experimental and predicted values.

Runs	Independent Variables			Dependent Variables	
	A	B	C	Y (exp.)	Y(pred.)
R1	80	7	15	27	29
R2	50	7	10	59	58
R3	20	7	15	69	70
R4	50	7	10	57	58
R5	20	11	10	60	60
R6	20	3	10	90	91
R7	20	7	5	72	67
R8	80	7	5	70	66
R9	80	11	10	30	29
R10	80	3	10	80	80
R11	50	11	15	42	36
R12	50	11	5	47	53
R13		3	15	79	78
R14	50	3	5	95	94
R15	50	7	10	55	58

A= Amount of polymer (in composite, % by weight); B= pH; C= CIP initial concentration (mg/L); Y= CIP removal (%)

Table 3: ANOVA results for Box-Behnken Design.

Source	DF	Adj SS	Adj MS	F-Value	P-Value
Model	6	5533.88	922.31	52.31	0.000
Linear	3	4846.25	1615.42	91.62	0.000
A	1	882.00	882.00	50.02	0.000
B	1	3403.13	3403.13	193.01	0.000
C	1	561.13	561.13	31.82	0.000
Square	1	187.63	187.63	10.64	0.011
B*B	1	187.63	187.63	10.64	0.011
2-Way Interaction	2	500.00	250.00	14.18	0.002
A*B	1	100.00	100	5.67	0.044
A*C	1	400.00	400	22.69	0.001
Error	8	141.05	17.63		
Lack-of-fit	6	128.39	21.40	3.38	0.246
Pure Error	2	12.67	6.33		
Total	14	5674.93			

A= Amount of polymer (in composite, % by weight); B= pH; C= CIP initial concentration (mg/L); Y= CIP removal (%)

According to the experimental design results, the increase in the TiO_2 ratio in the composite positively affected the CIP removal performance up to a certain value. However, when a composite with a TiO_2 content above a certain value is used, this effect decreases due to the turbidity that occurs. For this reason, the C50 composite was chosen as the best option.

When the effect of pH is examined, it was seen that the best results were achieved at pH=3. At this pH, while the catalyst surface was negatively charged, CIP is in cationic form and degradation performance improved due to electrostatic interactions between them.

When the experimental design results are evaluated, it was seen that the degradation efficiency decreased as the initial drug concentration increased. There are many possible reasons for this situation. One is that increasing concentration shortens the photon path entering the solution, resulting in lower photon adsorption on the catalyst particles. For this reason, the formation of hydroxyl radicals decreases and the photodegradation efficiency decreases. On the other hand, the probability of reaction increases as the concentration decreases. While the active sites on the photocatalyst surface can easily interact with the few CIP molecules in the medium, otherwise, only a part of the CIP can interact with the surface due to the excess in the medium with an increase in concentration. Thus, increasing in the concentration decreases the degradation efficiency.

4. Conclusions

In this study, composites were successfully synthesized using PS and TiO_2 at different ratios. This has been confirmed by XRD, FTIR, SEM and EDAX analysis. The usage of these composites as photocatalysts in the removal of CIP from wastewater by photocatalytic degradation was investigated. Optimum parameters of the process were determined by experimental design studies. Predictions made using the equation resulting from the design and the experimental results were compared and it was seen that they were very close to each other. This shows that the model represents the process well. The maximum removal percentage in this study was achieved using the C50 composite at pH 3 and an initial drug concentration of 5mg/L. In the light of these results, it was concluded that C50 could be used as a catalyst for CIP removal.

References

1. Shehu Imam, S., Adnan, R. & Mohd Kaus, N. H. Photocatalytic degradation of ciprofloxacin in aqueous media: a short review. Toxicological and Environmental Chemistry vol. 100 518–539 Preprint at https://doi.org/10.1080/02772248.2018.1545128 (2018).
2. Martins, P. et al. Enhanced photocatalytic activity of au/TiO2 nanoparticles against ciprofloxacin. Catalysts 10, (2020).
3. Malakootian, M., Nasiri, A. & Amiri Gharaghani, M. Photocatalytic degradation of ciprofloxacin antibiotic by TiO2 nanoparticles immobilized on a glass plate. Chem Eng Commun 207, 56–72 (2020).
4. Li, W. et al. Bi2Ti2O7/TiO2/RGO composite for the simulated sunlight-driven photocatalytic degradation of ciprofloxacin. Mater Chem Phys 256, (2020).
5. Hassani, A., Khataee, A. & Karaca, S. Photocatalytic degradation of ciprofloxacin by synthesized TiO2 nanoparticles on montmorillonite: Effect of operation parameters and artificial neural network modeling. J Mol Catal A Chem 409, 149–161 (2015).
6. Parmar, N. & Srivastava, J. K. Process optimization and kinetics study for photocatalytic ciprofloxacin degradation using TiO2 nanoparticle: A comparative study of Artificial Neural Network and Surface Response Methodology. Journal of the Indian Chemical Society 99, (2022).
7. Hu, X. et al. Mechanisms underlying the photocatalytic degradation pathway of ciprofloxacin with heterogeneous TiO2. Chemical Engineering Journal vol. 380 Preprint at https://doi.org/10.1016/j.cej.2019.122366 (2020).
8. Singh, S., Mahalingam, H. & Singh, P. K. Polymer-supported titanium dioxide photocatalysts for environmental remediation: A review. Applied Catalysis A: General vols 462–463 178–195 Preprint at https://doi.org/10.1016/j.apcata.2013.04.039 (2013).
9. Altin, I. & Sökmen, M. Preparation of TiO2-polystyrene photocatalyst from waste material and its usability for removal of various pollutants. Appl Catal B 144, 694–701 (2014).
10. Das, S. & Mahalingam, H. Dye degradation studies using immobilized pristine and waste polystyrene-TiO2/rGO/g-C3N4 nanocomposite photocatalytic film in a novel airlift reactor under solar light. J Environ Chem Eng 7, (2019).
11. Salehi, I., Shirani, M., Semnani, A., Hassani, M. & Habibollahi, S. Comparative Study Between Response Surface Methodology and Artificial Neural Network for Adsorption of Crystal Violet on Magnetic Activated Carbon. Arab J Sci Eng 41, 2611–2621 (2016).
12. Das, S. & Mahalingam, H. Reusable floating polymer nanocomposite photocatalyst for the efficient treatment of dye wastewaters under scaled-up conditions in batch and recirculation modes. Journal of Chemical Technology and Biotechnology 94, 2597–2608 (2019).
13. Srinivasu, P., Singh, S. P., Islam, A. & Han, L. Novel approach for the synthesis of nanocrystalline anatase titania and their photovoltaic application. Adv Optoelectron 2011, (2011).
14. Wang, J., Yu, J., Zhu, X. & Kong, X. Z. Preparation of hollow TiO2 nanoparticles through TiO2 deposition on polystyrene latex particles and characterizations of their structure and photocatalytic activity. Nanoscale Res Lett 7, (2012).
15. Ahmed, A. A. et al. SEM morphological analysis of irradiated polystyrene film doped by a Schiff base containing a 1,2,4-triazole ring system. Appl Petrochem Res 9, 169–177 (2019).
16. Wanjale, S. et al. Surface tailored PS/TiO2 composite nanofiber membrane for copper removal from water. J Colloid Interface Sci 469, 31–37 (2016).
17. Jaleh, B., Madad, M. S., Tabrizi, M. F., Habibi, S., Golbedaghi, R., & Keymanesh, M. R. (2011). UV-degradation effect on optical and surface properties of polystyrene-TiO 2 nanocomposite film. Journal of the Iranian Chemical Society, 8, S161-S168.